Thermal Roughening and Deroughening at Polymer Interfaces in Electrophoretic Deposition

2 AUTHORS:

Frank Wallace Bentrem
Binary Services Group Sdn Bhd
28 PUBLICATIONS **71** CITATIONS

SEE PROFILE

Ras B Pandey
University of Southern Mississippi
246 PUBLICATIONS **1,763** CITATIONS

SEE PROFILE

Thermal Roughening and Deroughening at Polymer Interfaces in Electrophoretic Deposition

Frank W. Bentrem[*]

Marine Geosciences Division, Naval Research Laboratory, Stennis Space Center, MS 39529

Ras B. Pandey

Department of Physics and Astronomy, The University of Southern Mississippi, Hattiesburg, MS 39406-5046

(Dated: *February 2005*)

Thermal scaling and relaxation of the interface width in an electrophoretic deposition of polymer chains is examined by a three-dimensional Monte Carlo simulation on a discrete lattice. Variation of the equilibrium interface width W_r with the temperature T shows deroughening $W_r \propto T^{-\delta}$, with $\delta \sim 1/4$, at low temperatures and roughening $W_r \propto T^{\nu}$, with $\nu \sim 0.4$ at high temperatures. The roughening-deroughening transition temperature T_t increases with longer chain lengths and is reduced by using the slower segmental dynamics.

I. INTRODUCTION

Polymer chains and particulates of all shapes and sizes form deposits when they are driven towards a substrate. A continuous release and deposition of driven polymer chains may lead to a polymeric material with a well defined density at the substrate, a growing bulk, and an evolving interface[1]. The characteristics of polymer conformation and density at the substrate, bulk, and the interface depend on factors such as the nature of the segmental dynamics of the polymer chains, polymer-substrate and polymer-polymer interactions and their entanglement, molecular weight, temperature, type of medium, etc. Similar issues emerge if the polymer chains are driven by an electric field as in gel electrophoresis[2,3,4] and deposit on the pore boundary of the gel. Another example would be a surface coating resulting from polymer chains deposited under a pressure gradient such as in spin-coating. The applications of such electrophoretic (driven) deposition and fabrication processes are enormous with a vast list of challenging questions in a relatively large parameter space[5]. Using a discrete-lattice computer simulation model, we would like to focus here on the basic issue of how the interface roughness depends on temperature.

We know that, as the polymer chains deposit on an impenetrable substrate, the polymer density increases and the interface develops[6,7,8,9]. The fluctuation in the height (measured from the substrate) of the polymer coating along the longitudinal (i.e., growth) direction is the interface width W and is a measure of the surface roughness. The interface width is found to grow in time with power laws ($W = At^{\beta_1}$, Bt^{β_2}), where β_1 is the initial growth exponent followed by β_2)[7,8,10,11,12,13] before saturating to a steady-state (constant) value W_s in the asymptotic regime as the polymer chains continue to deposit. For the interface growth of particles (this could be viewed as the extreme limit of reducing the chain length) deposition[10,11,12], the saturation of the interface occurs as the height-height correlation length exceeds the substrate length. For the electrophoretic deposition of polymer, such a relation between the height-height correlation length and substrate length is less clear[7,8]. The problems become much more complex due to additional relevent lengths such as radius of gyration, complex density-density correlations (intra- and inter-chain), and their dependence on temperature, field, etc. In fact, we have observed interesting roughening and deroughening of the interface as various influences (driving mechanisms such as temperature and field[13]) compete and cooperate.

Recently it was found[13] that the steady-state interface width W_s may reduce to a lower value (W_r) if the system is relaxed by continuing segmental movements of existing chains without adding new chains into the system. We have noted contrast in the characteristics of the relaxed interface width W_r including its dependence on the molecular weight from that of the steady-state width W_s. In our previous study[13], we examined the effect of the driving field on the interface width. Dependence of the interface width and morphology on the temperature for particle deposition has been recently observed experimentally[14,15,16,17] as well as with Monte Carlo simulations[15,16,18]. In fact, the variation of the interface width with temperature is shown, under certain conditions, to be nonmonotonic[15,18]. Polymer surfaces are also affected by the deposition temperature[9,13,19]. In this article, we address the dependence of the interface width on the temperature using a variety of chain lengths, sample sizes and segmental dynamics after relaxing the polymer chains by "turning off" the source of new chains. In the following, we will briefly introduce the simulation model and follow with a discussion of the results and conclusions.

[*]To whom correspondence should be addressed.

II.   METHOD

We use our previous computer simulation model[8,13,20] on a discrete cubic lattice of size $100 \times L \times L$ with $L = 4$–40. This is a coarse-grained model with the charged polymer (polyelectrolyte) chains represented by a number of contiguous occupied lattice sites, each assigned a unit charge. The chains are initially placed near one end of the sample (near $x = 1$) by a self-avoiding walk and are then driven toward the substrate/wall at the opposite end ($x = 100$) by a field E. The length of a chain L_c is the number of lattice sites it occupies. For the simulations reported here, $L_c = 10$–200. In addition to excluded volume we consider nearest-neighbor and polymer-polymer repulsive interactions as well as polymer-wall attractive interactions. Two different combinations of segmental chain dynamics[21], kink-jump and crankshaft (KC) (slower)[22] and kink-jump, crankshaft, and reptation (KCR) (faster) are used to move the chains according to the Metropolis algorithm. The energy change for a chain segment due to the field is

$$\Delta U = E \Delta x,$$

where Δx is the displacement parallel to the field. The repulsive inter- and intra-chain (Coulombic) interaction and attractive polymer-substrate interaction is represented by the energy potential

$$U = J \sum_{ij} \rho_i \rho_j, \tag{1}$$

where $J = 1$, $\rho_i = 1$ for every occupied lattice site i, $\rho_i = 0$ for all unoccupied sites, and $\rho_i = -1$ for every site along the substrate ($x = 101$). The summation in eq 1 is over all nearest-neighbor sites in the lattice. An open boundary condition is used along the longitudinal (x) direction and a periodic boundary condition along the transverse (y,z) directions. An attempt to move each node once is defined as one Monte Carlo Step (MCS). One polymer chain is released into the sample every $32 L_c / L^2$ MCS for a constant deposition rate of 0.0005 monomer units per MCS per substrate lattice site. After 75,000 MCS, we allow the sample to relax by stopping the release of new chains but continuing to drive the remaining chains with the electric field until equilibrium is reached. The simulations are performed for many independent samples to calculate the average values of the physical quantities, i.e., density profile, interface width, radius of gyration, etc. Further, we have used different sample sizes to check for the finite size effects. Most of the data presented here were generated on a $100 \times 40 \times 40$ lattice with 10-20 independent simulations, and we have not noticed severe finite size effects on the qualitative nature of the physical quantities, except for low temperatures ($T < 0.3$). The unit for all length quantities is the lattice constant, and arbitrary units are used for the temperature and electric field.
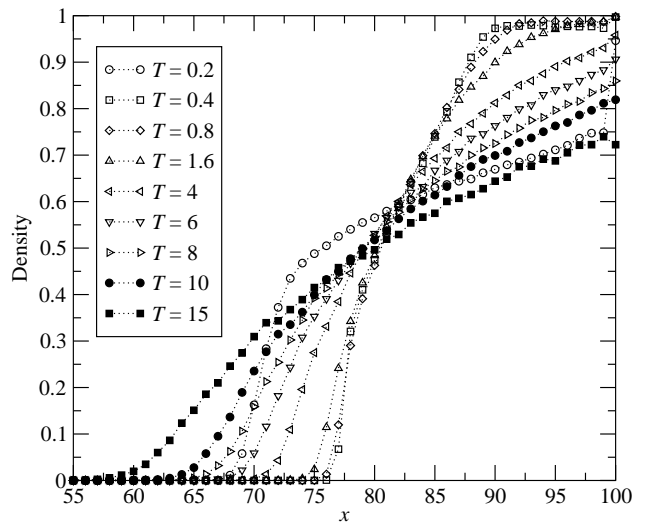

FIG. 1: Density profile using a combination of kink-jump and crankshaft (KC) segmental dynamics. The sample size is $100 \times 40 \times 40$ with $L_c = 40$ and $E = 0.5$ at various temperatures (in arbitrary units) for 10–20 independent samples. Density is the fraction of occupied lattice sites and x has units of the lattice constant.

III.   RESULTS

Figure 1 shows the equilibrium density profile with the KC dynamics at different temperatures with $E = 0.5$ and $L_c = 40$. Note that the shape of the density profile depends on the temperature. It is worth pointing out that we have also carried out our simulations at lower temperature (i.e., $T < 0.1$) with KC dynamics, but encountered technical problems, namely clogging, before deposition and a long relaxation time. On the other hand, the interface width (along with all other physical quantities such as density profile, radius of gyration, etc.) has reached equilibrium at all temperatures we have studied with the fastest (KCR) dynamics. The shape of the density profiles using KCR dynamics is similar to those in Figure 1.

The interface width is defined by

$$W^2 = \frac{\sum_i (h_i - \overline{h}_i)^2}{L^2},$$

where h_i is the distance in units of the lattice constant from the substrate lattice site i to the deposited polymer farthest from the substrate (in the same y-z column) and $\overline{h}_i$ is the average distance from the substrate. Variation of the interface width with time (in Monte Carlo Steps) for KCR dynamics is presented in Figure 2. We see that the initial power-law growth of the interface width ($W \propto t^\beta$) is followed by a steady-state value after 10^4 MCS. After 7.5×10^4 time steps, the steady-state interface width W_s is allowed to relax to its equilibrium value W_r (by ceasing to release new polymer chains into the system) as in Figure 3. Results are qualitatively similar for the KC segmental dynamics. Note that the relaxation to equilibrium occurs rapidly except at high tem-
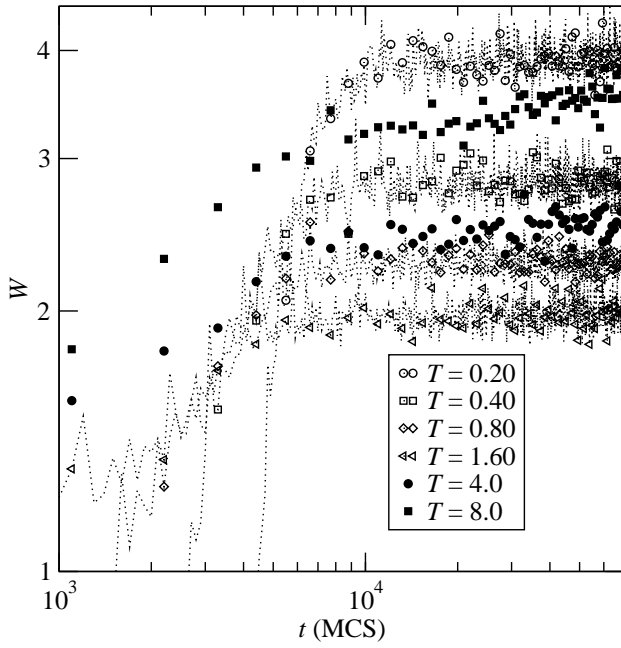
FIG. 2: Interface width W (in units of the lattice constant) versus time steps t before surface relaxation on a log-log scale using KCR segmental dynamics for selected temperatures (in arbitrary units) and 10–20 independent samples. Other parameters are the same as in Figure 1.
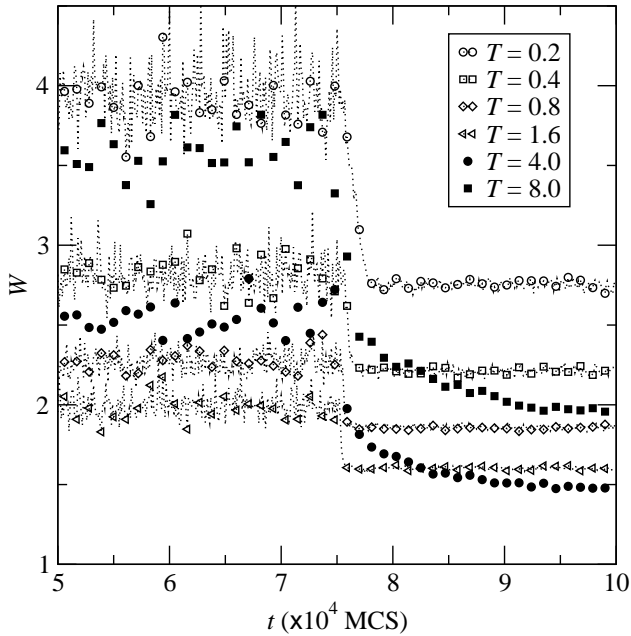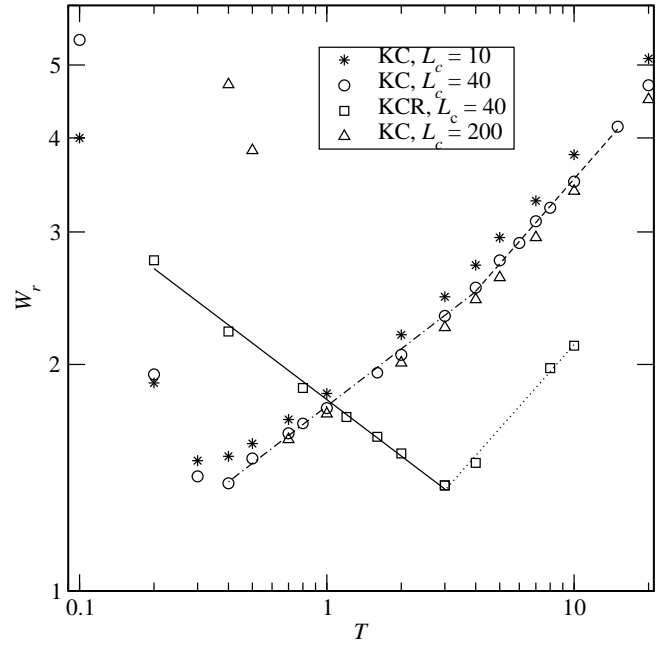

FIG. 4: Equilibrium (relaxed) interface width W_r (in units of the lattice constant) versus T using KC, and KCR (squares) segmental dynamics with $E = 0.5$. Different chain lengths are used with the KC dynamics. Other parameters are the same as in Figure 1. The solid line shows the power-law decay (eq 2) with $\nu = -0.25$ The dotted, dashed, and dotted-dashed lines show the power-law growths (eq 3) with $\delta =0.37$, 0.38, and 0.25, respectively. Temperature T and E are in arbitrary units.

FIG. 3: Interface width W (in units of the lattice constant) versus time steps t at later times showing surface relaxation. The simulations used KCR segmental dynamics for different temperatures (in arbitrary units) and 10–20 independent samples. Other parameters are the same as in Figure 1.
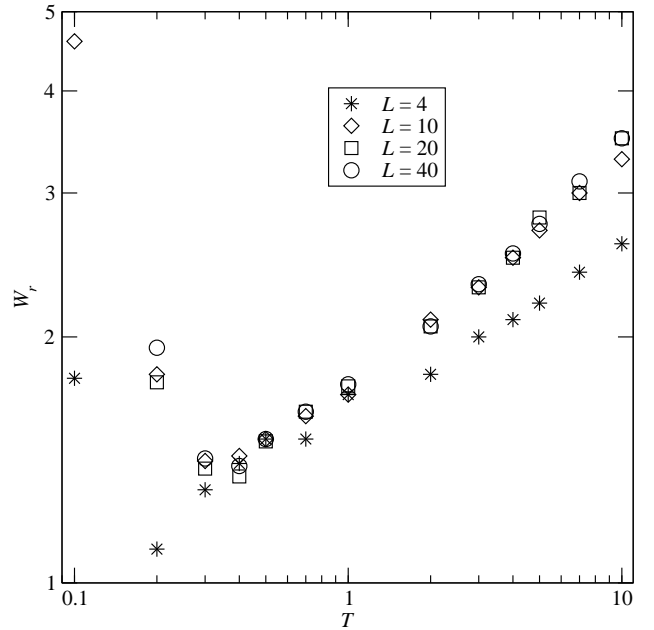

FIG. 5: Equilibrium (relaxed) interface width W_r (in units of the lattice constant) versus T using a variety of sample sizes ($L = 4$–40) with KC (circles) segmental dynamics and $E = 0.5$. Other parameters are the same as in Figure 1. Temperature T and E are in arbitrary units.

TABLE I: Transition Temperatures T_t at $E = 0.5$

L_c	L	dynamics	T_t
40	4	KC	0.20
40	10	KC	0.34
40	20	KC	0.36
40	40	KC	0.35
10	40	KC	0.32
200	40	KC	0.7
40	40	KCR	3.0

peratures ($T = 4.0, 8.0$). Figure 4 shows the variation of the equilibrium interface width W_r with the temperature on a log-log scale using KC and KCR segmental dynamics. For KC dynamics in the high temperature regime ($T \geq 4.0$), W_r shows a power-law scaling,

$$W_r \propto T^\nu, \qquad (2)$$

where $\nu \sim 0.4$. At low temperatures, on the other hand, there is a tendency for W_r to decay with temperature. With KCR dynamics, we see a power-law decay,

$$W_r \propto T^{-\delta}, \qquad (3)$$

where $\delta \sim 1/4$. Thus, there is a power-law scaling for the roughening of the equilibrium width W_r at high temperature and deroughening at low temperatures. For $L_c = 40$ the roughening-deroughening transition temperature for KC dynamics ($T_t \approx 0.35$) is lower than for KCR dynamics, where $T_t \approx 3.0$. On the other hand, the reduced mobility of longer chains results in an increase in the transition temperature so that $T_t \approx 1.8$ for $L_c = 200$ while $T_t \approx 0.32$ for $L_c = 10$. To investigate finite-size effects we vary the sample size $L = 4$–40 and plot the temperature dependence of the interface width in Figure 5. For moderate temperature ($T = 0.4$–1.0), no significant finite-size effects are observed. At higher temperatures, thermal mobility increases the lateral height-to-height correlation length, which limits the interface width for small sample sizes ($L = 4$). The transverse (y, z) components of the polymer chains' radius of gyration increases at low temperatures[23], which leads to definite finite-size effects. The transition temperatures are summarized in Table I.

It is also of interest to compare the temperature dependence of the steady-state (W_s) and equilibrium (W_r) interface widths. Figure 6 shows their variation with temperature for KC dynamics. We see that the nonmonotonic dependence of W_s on the temperature is qualitatively similar to that of W_r with the faster KCR dynamics. Scaling of W_s with T is perhaps more complex than a single power-law as for W_r.

Even for simpler particle surfaces there exists a complex temperature dependence for roughness with several mechanisms[15], yet the thermal scaling observed in our polymer interface simulations is even more complex due to the many degrees of freedom for the chains. At low temperatures we can expect an increase in temperature to facilitate lateral (intralayer) diffusion[15] with relatively
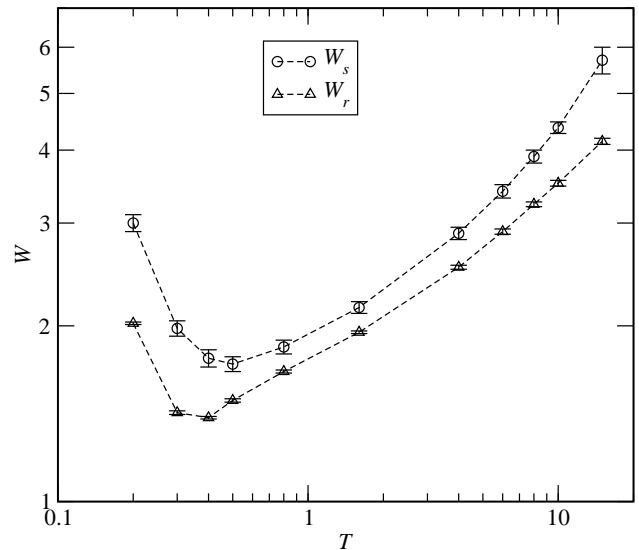
FIG. 6: Interface width (W_s and W_r, in units of the lattice constant) versus T (in arbitrary units) with KC segmental dynamics. The parameters are the same as in Figure 1.

less constraint due to entanglement. This will allow the polymer chains to reach a lower energy configuration (smoother interface). At temperatures above the roughening-deroughening temperature, azimuthal (interlayer) diffusion dominates, and constraint due to entanglement becomes more pronounced creating a (rougher) dynamic interface.

IV. CONCLUSION

In summary, the relaxation of the polymer chains, density, and interface width depend on the segmental dynamics as well as the temperature. The combination of slow-to-fast segmental dynamics (KCR) seems to rather effectively equilibrate the system in our observation time. Simulation with the slower KC dynamics at very low temperatures, while not very efficient for reaching equilibrium, provides insight into the nature of relaxation and the effects of clogging. However, we do not know which segmental dynamics is more appropriate for comparison with any given laboratory measurements, though we are able to make some important scaling predictions: the equilibrium interface width W_r shows roughening with the temperature, $W_r \propto T^{0.4}$ in the high temperature regime and deroughening $W_r \propto T^{-1/4}$ at low temperatures (at least with KCR segmental dynamics). The transition temperature T_t that separates the roughening and deroughening regimes depends on the polymer chain length and segmental dynamics. The steady-state interface width (W_s) also exhibits a nonmonotonic dependence on temperature, i.e., deroughening at low temperatures followed by roughening at high temperatures with both KC and KCR dynamics.

[1] Wool, R. P. In *Polymer Interfaces: Structure and Strength*; Hanser Publishers: New York, 1995.

[2] Andrews, A. T. In *Electrophoresis: Theory, Techniques, and Biochemical and Clinical Applications*; Clarendon Press: Oxford, 1981.

[3] Hoagland, D. A.; Smisek, D. L.; Chen, D. Y. *Electrophoresis*, **1996**, *17*, 1151.

[4] Perkins, T. T.; Smith, D. E.; Chu, S. *Science* **1997**, *276*, 2016.

[5] Van der Biest, O. O.; Vandeperre, L. J.; *Annu. Rev. Mater. Sci.* **1999**, *29*, 327.

[6] Foo, G. M.; Pandey, R. B. *J. Chem. Phys.* **1997**, *107*, 10260.

[7] Foo, G. M.; Pandey, R. B. *Phys. Rev. E* **2000**, *61*, 1793.

[8] Bentrem, F. W.; Pandey, R. B.; Family, F. *Phys. Rev. E* **2000**, *62*, 914.

[9] Pandey, R. B.; Urban, M. W. *Langmuir* **2004**, *20*, 2970.

[10] Halpin-Healy, T.; Zhang, Y.-C. *Phys. Rep.* **1995**, *254*, 215.

[11] Barabási, A.-L.; Stanley, H. E. In *Fractal Concepts in Surface Growth*; Cambridge University Press: Cambridge, 1995.

[12] *Dynamics of Fractal Surfaces*; Family, F.; Vicsek T., Eds.; World Scientific: Singapore, 1991.

[13] Bentrem, F. W.; Xie, J.; Pandey, R. B. *Phys. Rev. E* **2002**, *65*, 041606.

[14] Setzu, S.; Lérondel, G.; Romestain, R. *J. App. Phys.* **1998**, *84*, 3129.

[15] Stoldt, C. R.; Caspersen, K. J.; Bartelt, M. C.; Jenks, C. J.; Evans, J. W.; Thiel, P. A. *Phys. Rev. Lett.* **2000**, *85*, 800.

[16] Caspersen, K. J.; Stoldt, C. R.; Layson, A. R.; Bartelt, M. C.; Thiel, P. A.; Evans, J. W. *Phys. Rev. B* **2001**, *63*, 085401.

[17] Zhang, B. P.; Wakatsuki, K.; Binh, N. T; Usami, N.; Segawa, Y. *Thin Solid Films* **2004**, *449*, 12.

[18] Kalke, M.; Baxter, D. V. *Surface Science* **2001**, *477*, 95.

[19] Lee, S. H.; So, M. G. *J. Mat. Sci.* **2000**, *35*, 4789.

[20] Bentrem, F. W.; Xie, J.; Pandey, R. B. *J. Mol. Struct.* **2002**, *592*, 95.

[21] *Monte Carlo and Molecular Dynamics Simulations in Polymer Science*; Binder, K., Eds.; Oxford University Press: New York, 1995.

[22] Verdier, P. H.; Stockmayer, W. T. *J. Chem. Phys.* **1962**, *36*, 227.

[23] Bentrem, F. W. *Growth of Polymer Films by Driven Deposition: Monte Carlo Simulations* Dissertation, The University of Southern Mississippi, 2004.